Optimization and Engineering (2022) 23:1677–1705
https://doi.org/10.1007/s11081-021-09682-4

RESEARCH ARTICLE

Underground production scheduling with ventilation and refrigeration considerations

Oluwaseun Ogunmodede[1] · Patricio Lamas[2] · Andrea Brickey[3] · Gregory Bogin Jr.[1] · Alexandra Newman[1]

Received: 7 February 2021 / Revised: 15 August 2021 / Accepted: 15 August 2021 / Published online: 13 January 2022

Abstract

Underground mine production scheduling determines when, if ever, activities associated with the extraction of ore should be executed. The accumulation of heat in the mine where operators are working is a major concern. At the time of this writing, production scheduling and ventilation decisions are not made in concert. Correspondingly, heat limitations are largely ignored. Our mixed-integer program maximizes net present value subject to constraints on precedence, and mill and extraction capacities with the consideration of heat using thermodynamic principles, while affording the option of activating refrigeration to mitigate heat accumulation. In seconds to hours, depending on the problem size (up to thousands of activities and 900 daily time periods), a corresponding methodology that exploits the mathematical problem structure provides schedules that maintain a safe working environment for mine operators; optimality gaps are no more than 15% and average less than half that for otherwise-intractable instances.

Keywords Underground mine scheduling · Integer programming applications · Resource-constrained project scheduling · Ventilation · Diesel equipment · Refrigeration

1 Introduction and literature review

Underground mine production scheduling determines a sequence of activities associated with the extraction of deep crustal rock containing economic quantities of metal or minerals, called ore. Rock without sufficient economic value is referred to as waste. Underground mining is most often used when costs or safety factors

✉ Alexandra Newman
anewman@mines.edu

Extended author information available on the last page of the article

prohibit accessing the ore deposit from the surface (Hartman and Mutmansky 2002). Although more expensive on a unit-cost basis than surface mining, underground mining methods tend to provide greater ore selectivity with reduced waste extraction. The accumulation of heat in an underground mine is a major concern for operators. At the time of this writing, production scheduling decisions largely ignore the accumulation of heat. We propose a mixed-integer program that maximizes net present value subject to constraints on precedence, and mill and extraction capacities with the consideration of heat using thermodynamic principles; we add the option of activating refrigeration to mitigate heat accumulation. Although we present a deterministic model in which various sources of uncertainty, e.g., heat levels, are largely ignored, our contribution lies in the fact that, to our knowledge, this is the first piece of research that combines heat, ventilation, refrigeration, and large-scale, long-term scheduling in underground mine planning. We further demonstrate, via realistic case studies, that our solutions provide expected heat accumulation levels based on the mitigation employed.

1.1 Introduction

Many factors influence the size and scale of an underground mine including: geology, deposit type, geotechnical characteristics, and economics. Through mine planning processes, engineers must determine how the deposit will be: *(1)* accessed, e.g., via a vertical shaft or decline; *(2)* mined, i.e., according to which mining method; *(3)* transported, e.g., employing equipment and/or hoists; and, *(4)* remediated, e.g., by using backfill. These decisions are based on commodity prices, mining costs, physical limitations, operational parameters, and health and safety factors (Gertsch and Bullock 1998).

Underground mines utilize shafts or declines, i.e., ramps, to provide access from the surface. Connected to the main access infrastructure, drifts and haulage ways provide ingress to the ore deposit. Once mining has begun, ore is transported via trucks, trains, or conveyor belts, to the shaft or decline and then to the surface. Figure 1 shows common underground mine design elements, such as: *(i)* major access infrastructure; *(ii)* production stopes, i.e., areas within the orebody where ore is extracted, leaving a void after extraction; *(iii)* drifts and haulage levels, which are underground openings that allow mining equipment to transport material throughout the mine; and, *(iv)* backfilled stopes, which are previously mined areas that are filled with waste or a processing by-product used to maintain structural integrity. In addition, most metallic ores require processing to extract the desired metal, or to remove unwanted minerals or metals contained in the rock, before the final product can be sold.

The choice of an appropriate mining method is based on numerous factors such as ore strength, depth, shape, and size, among other characteristics unique to each deposit (Nieto 2011). This study focuses on two bulk mining methods, sublevel stoping and sublevel caving, which have limited selectivity and are therefore associated with higher production rates and lower unit operating costs than their more selective counterparts. Sublevel stoping, see Fig. 2a, consists of developing access to stopes, i.e., areas where ore is drilled, blasted, and then extracted using mechanical equipment. Once the broken ore is extracted and transported to the

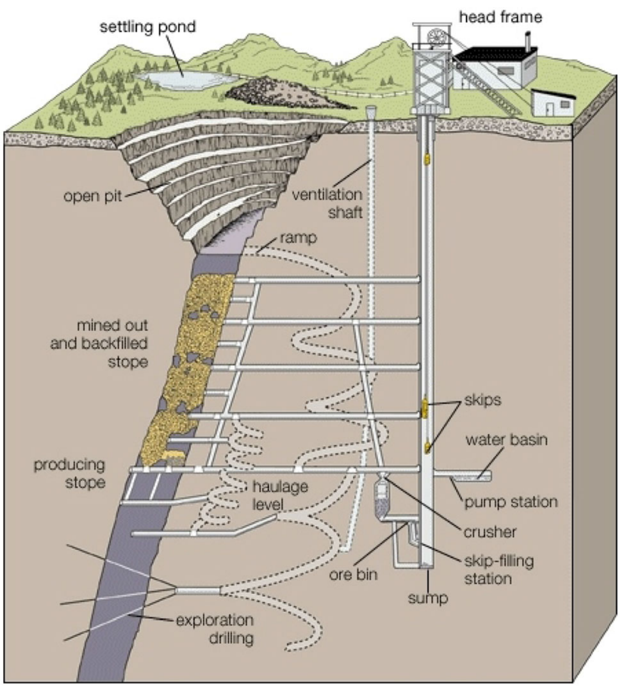

Fig. 1 Diagram of an open pit and underground mine (reused with permission from Epiroc: Hamrin (1980))

surface, the resulting void may be backfilled, i.e., filled with waste rock or processing waste, to provide ground support or as a depository for waste rock. Sublevel caving is similar to sublevel stoping with one significant discrepancy; the ore is blasted but the surrounding waste rock is allowed to cave (Fig. 2b), yielding a higher production rate relative to that of sublevel stoping. The ability to cave requires specific geologic conditions, and surface subsidence can prevent its employment. For both methods, stopes, i.e., mining areas, are defined using economic and engineering factors. Stope size, layout, and number of active mining areas can have a positive correlation with production rates, i.e., more active mining areas often result in higher production rates. For additional information on underground mining methods, please refer to Hustrulid and Bullock (2001).

The process of determining the sequence of activities in a mine is termed *mine planning*, and is based on information resulting from geologic resource models, mine layout, infrastructure, revenues and costs. Various scenarios that depend on the detail in the input data, the time fidelity, e.g., months, and the time horizon, e.g., years, are evaluated at different stages of the mine's development to make and, subsequently, execute critical decisions impacting the productivity, safety, and efficiency of the mine. Underground mining presents many occupational hazards (Donoghue 2004) such as harmful gases from blasting activities, particulates from combustion engines, and heat from a variety of sources. In particular, as mines extend deeper underground, naturally occurring heat from geothermal sources,

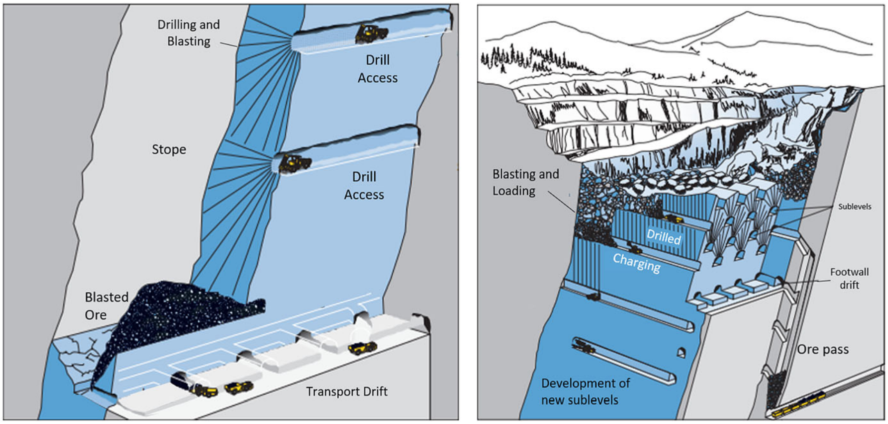

(a) Diagram of sublevel stoping mining **(b)** Diagram of sublevel caving mining

Fig. 2 Diagrams of the two different mining methods (reused with permission from Epiroc: Atlas Copco (2007))

equipment, auto-compression (resulting from the fact that air at lower elevations is more dense), and other sources causes the air temperature to rise. Heat from internal combustion engines, i.e., mining equipment used to transport rock from the mining area to the surface, can add both heat and humidity to the mine air (Hartman et al. 2012; McPherson 2012). The physiological effects of heat exposure can create a health hazard and must be controlled to protect working miners. To provide a safe environment, underground mines utilize mechanical fans to push or pull air through the infrastructure network. Lazaro and Momayez (2020) provide a thorough review of the impacts of heat stress.

Ventilation in underground mines can be modeled as a network, where the source node marks the intake and the terminal node signifies the outlet. The workings, e.g., tunnels, of the underground mine are represented by arcs, and the junctions correspond to nodes (De Souza 2007). Figure 3 provides a simplified diagram, the more complicated rendition of which consists of one or more primary, i.e., main, fans located on the surface or underground. Primary fans provide the air flowing through the ventilation network. Auxiliary fans, unlike primary fans, help to direct air to active working areas which are difficult to reach without additional mechanical power (McPherson 2009). Once a ventilation system, i.e., the network of infrastructure and mechanical fans, is constructed and operational, achieving additional airflow, or conditioning the air, may require large capital investments and necessitate additional infrastructure, e.g., fans and ventilation shafts. Air conditioning can include changing the air temperature or removing humidity before the air flows through the mine. To decrease the temperature, the intake air can be cooled via refrigeration, a supplement to mine ventilation. However, refrigeration plants are expensive and inflate the already-high costs of mine ventilation (Greth et al. 2017). Additionally, refrigeration may not be needed at the beginning of the

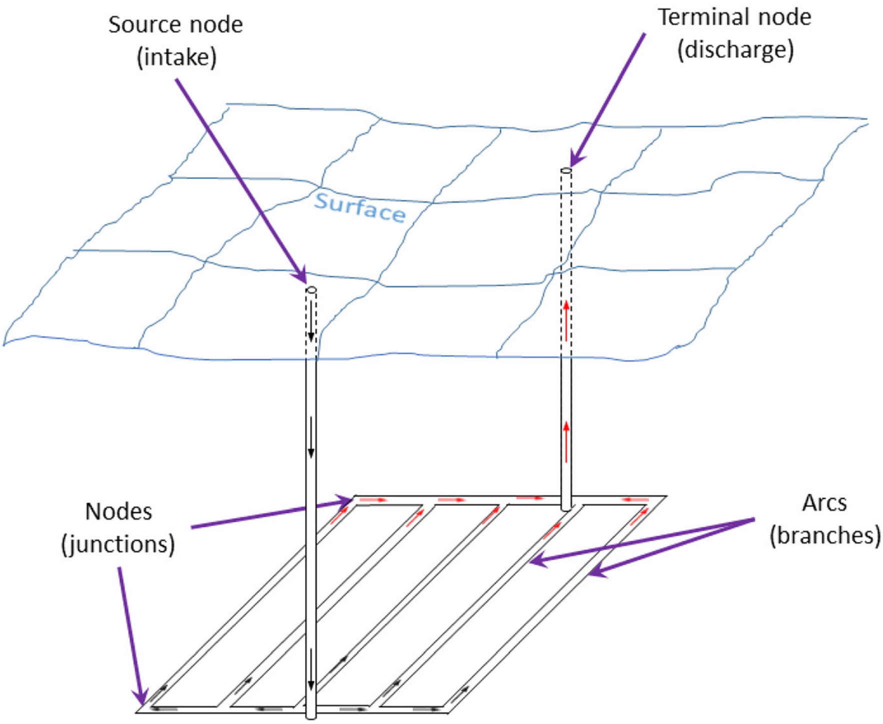

Fig. 3 Diagram of a basic ventilation network (reused with permission from the creator: Larson (2021))

operation but is required as the mine descends beneath the surface. This evolving challenge requires planning to ensure that refrigeration components are constructed and operational in a timely fashion. In some cases, refrigeration may be installed in stages, where each stage increases the total refrigeration capacity of the system.

We show the impact of incorporating ventilation and refrigeration constraints on production schedules and, in so doing, extend Brickey (2015)'s work, which focuses on ventilation with respect to the dilution of diesel particulate matter in an airway. However, unlike that work, we consider heat, rather than diesel particulate matter, to constitute the "nuisance," based on industrial concerns from certain operational mines. Specifically, we consider heat in a detailed computational analysis used to inform the constraint set of our integer program.

1.2 Literature review

Operations research has been used in mining since the 1960's, with most early research directed towards the open pit variant (Lerchs and Grossmann 1965; Johnson 1968). Overall, activities in underground mines are much more difficult to schedule than those of their open-pit counterparts, because of their heterogeneous nature (with respect to duration, precedence relationships and resources required for their execution), increased geotechnical risk associated with accessing the ore, and additional protocols necessary for safe operations (O'Sullivan et al. 2015). As demand for more detailed mine plans increases, commensurate advances in algorithms and computational power provide more accurate and more robust production schedules.

Until the early 2000s, underground production scheduling models given in the academic literature were mine-specific. Trout (1995) provides one of the first templates of underground production scheduling for a sublevel stoping operation known as Mt. Isa in Australia. Carlyle and Eaves (2001) adapt Trout's work to a hardrock mine in Stillwater, Montana in which development, drilling, and other preparation activities are scheduled. Smith et al. (2003) implement a mixed integer program for a life-of-mine schedule at Mt. Isa that significantly reduces solution times by aggregating time periods; the result, while not provably optimal, demonstrates significant improvement in net present value over those generated via traditional spreadsheet-based methods. LKAB's Kiruna sublevel caving mine in Sweden has used models that implement variable reduction, aggregation, and decomposition techniques to improve tractability (Kutcha et al. 2003; Kuchta et al. 2004; Newman and Kuchta 2007; Martinez and Newman 2011). These consider details of the operation such as electric tethered load-haul-dump trucks, which limit the amount of equipment with power cables operating in a given area, as well as precedence constraints between so-called machine placements, to minimize the deviation between iron ore produced in each time period and that set by long-term contracts. O'Sullivan and Newman (2014) do the same for an Irish lead and zinc mine, and Lopes (2017) applies a sliding time window heuristic to obtain solutions for a hardrock mine.

Researchers are increasingly solving medium- and short-term models with a commensurate level of detail. Nehring et al. (2010) provide a production scheduling model that integrates long- and short-term scheduling by: (*i*) considering the net present value of activities, and (*ii*) taking into account the deviation between when these activities start relative to a predetermined target date. Similarly, Nehring et al. (2012) explore the integration of medium- and short-term planning in underground mining. Although Nehring et al. use a small test case to evaluate the model, such tests highlight the importance of incorporating an increased level of detail. Other authors include the impact of human and technical factors, such as number of teams, team efficiencies, and team size, that can affect productivity (Sebutsoe and Musingwini 2017); active mining levels available for simultaneous extraction or advancement (Huang et al. 2020a); ore mixed near adjacent drawpoint columns (Khodayari and Pourrahimian 2019); and, the availability of mining equipment as a resource (Campeau and Gamache 2020).

The afore-mentioned models are deterministic, but mine planning is subject to financial, geological, and geotechnical uncertainty. Myers et al. (2005) and

Dimitrakopoulos and Grieco (2009) examine an underground stoping mine, the latter analyzing alternative designs. Jewbali et al. (2015) perform evaluations under resource uncertainty. Carpentier et al. (2016) consider geological uncertainty while accounting for standard aspects such as precedence constraints, production capacity, and processing limits, but also material handling flow conservation. Tavchandjian et al. (2018) examine capital investment decisions using conditional simulation. Dirkx et al. (2019) study delay associated with geotechnical uncertainty and ore grade variation related to geological uncertainty for an underground caving operation; specifically, the authors incorporate these sources of stochasticity into a production plan and use a sliding time window solution approach to compare their results verus overly optimistic deterministic-equivalent solutions. Huang et al. (2020b) extend earlier work on a cut-and-fill underground mine (Huang et al. 2020a) to maximize net present value while minimizing deviation from production targets using a stochastic programming framework.

Finally, some authors examine the effects of uncertainty on mine planning, taking into account the way in which the equipment is employed (Matamoros and Dimitrakopoulos 2016); here, the authors consider a short-term planning scenario in an open pit mine using a small case study that precludes the necessity of a novel solution technique. Both and Dimitrakopoulos (2020) propose a metaheuristic to simultaneously determine a production and fleet schedule under geologic uncertainty, also for short-term planning in an open-pit mine; both shovel haulage and truck allocation are considered, and Mohtasham et al. (2021) confront a similar problem using a chance-constrained goal program. Our model's setting is an underground, rather than an open-pit, mine, and obviates the detailed consideration of equipment use because we address tactical, rather than short-term, decisions.

Nesbitt et al. (2021) consider both financial and geotechnical uncertainty in a tactical, underground mine planning environment (without equipment decisions). Using a standard model of maximizing net present value subject to precedence and resource constraints, they exploit a so-called *resource-constrained project scheduling problem* structure to enable the solution of large (at the time of this writing) stochastic instances, i.e., containing nearly 5,000 activities and 1,000 days – employing daily time fidelity. Algorithms whose details are contained in Bienstock and Zuckerberg (2010) to solve the linear programming relaxation, and Rivera Letelier et al. (2020) for the corresponding rounding heuristic (that yields integer-feasible solutions) accommodate instances with five scenarios.

In none of the afore mentioned references is ventilation explicitly incorporated. Marks (1980) and Brake and Fulker (2000) examine ventilation, and the refrigeration layout, using economic cost-benefit analysis; although their studies advance the understanding of ventilation, they fail to consider operational factors or the integration of refrigeration and production scheduling. Magri and Unsted (1976) and Anderson and Longson (1986) provide numerical methods to appropriately size ventilation and refrigeration for an underground mine. Specifically, the former research introduces a mixed integer programming model to evaluate ventilation and refrigeration costs for a given production schedule; the latter work is a simulation model. However, neither considers all heat sources; specifically, they omit that from diesel machinery.

Sotoudeh et al. (2020) provide an overview in which sublevel stoping is the primary underground mining method. The authors encourage researchers to focus on extending optimization models to include more detail, thereby increasing the operational feasibility and accuracy of the resulting solutions. While there is significant literature on ventilation and production scheduling in underground mining, there is sparse literature integrating the two topics. Sotoudeh et al. suggest that the combination is considered by only a few researchers, e.g., Brickey (2015); Sharma (2015) and Zhang et al. (2017). Brickey and Sharma both treat airflow as a resource which is limited per time period. Brickey extends this concept by assigning domains based on the location of the respective activities. Zhang et al. explore the effects that certain activities have on air flow availability in a long-term schedule. It is with this perspective that we propose our model and corresponding solution methodology. Owing to the ensuing complexity, we address a deterministic version. Extending the work using concepts from Nesbitt et al. (2021) to incorporate stochasticity is outside the scope of this paper, but provides an interesting and challenging extension. More detail regarding state-of-the-art modeling in underground production scheduling can be found in Newman et al. (2010), Acuña and Lowndes (2014), and Chowdu et al. (2021).

The remainder of this paper is organized as follows: Section 2 highlights the heat considerations in underground mining. Section 3 details the initial model formulation. Section 4 explains the solution methodology, which, inter alia, involves model reformulation. Section 5 analyzes results, and Section 6 concludes and suggests future work.

2 Underground mine ventilation

In order to mitigate the unacceptable work conditions associated with high temperatures, and to better approximate realistic production schedules, we first develop a framework in which we can characterize heat sources in underground mines. Heat dissipates both temporally and spatially during mining operations. We define an activity as a type of work, e.g., development, mucking, extraction, executed in a fixed location in space; as such, an activity is associated with equipment types, durations, and timing, as well as with a given tunnel of the mine. As an activity is executed, heat is emitted, which then travels to other sections over time, increasing the ambient air temperature. A *heat load* is defined as the heat transfer rate from one body to another. Three main sources are the following: *(i)* diesel equipment, *(ii)* auto-compression, and *(iii)* strata rock. We discuss how each of these sources is modeled, calculated, and handled, given the following assumptions: *(i)* the model into which the heat is incorporated is solved at steady state, implying that heat from the previous time period does not inform the heat output for the current time period; *(ii)* the mass flow rate, $\dot{m}$, is constant on each mine level n; *(iii)* the air flow velocity is constant, provided that there are auxiliary fans on each level; *(iv)* the relative humidity is constant throughout the mine; and, *(v)* sensible heat from equipment is absorbed into the air via convection on any given mine level. We note that the greatest observed mode of heat transfer is convection (relative to conduction and radiation). Blasting operations, i.e., the use of explosives to break rock, are a source of heat, yet much of the heat created during the detonation is expelled from the mine in the gasses produced by the blast. Some heat is transferred to the strata and dissipates over time; however, the air used to ventilate blasted areas after detonation is not used to support other active mining areas. In addition, the heat generated from blasting is negligible relative to that from other sources (specifically, 10% at most); therefore, we exclude blasting as a heat source. We use the following notation to mathematically model the heat in the mine:

Symbol	Explanation	Units
Simple Sets		
$\mathcal{A}$	Activities	
$\mathcal{C}$	Cycle stages	
$\mathcal{E}$	Equipment	
$\mathcal{N}$	Mine levels	
Indexed Sets		
$\tilde{\mathcal{A}}_n \subset \mathcal{A}$	Activities occurring on mine level n	
$\mathcal{C}_{en} \subset \mathcal{C}$	Cycle stages for equipment e on mine level n	
$\mathcal{E}_a \subset \mathcal{E}$	Equipment required for activity a	
Parameters		
c_p	Specific heat capacity of the air	$\left[\frac{J}{kg\cdot{}^\circ C}\right]$
k	Thermal conductivity of the mine rock	$\left[\frac{W}{m\cdot{}^\circ C}\right]$
l_n	Length of mine level n	$[m]$
$\hat{p}_{ea}$	Proportion of time equipment e is used for activity a	$[-]$
$\widehat{p}_{ecn}$	Proportion of time equipment e is used for cycle stage c on mine level n	$[-]$
p_n	Perimeter along the length of mine level n	$[m]$
$\dot{q}_a$	Heat load for activity a	$[W]$
$\ddot{q}_{en}$	Heat load for equipment e in mine level n	$[W]$
$\dddot{q}_{ecn}$	Heat load for equipment e during cycle stage c on mine level n	$[W]$
$\dot{q}_n^{\mathrm{v}}$	Virgin rock heat load on mine level n	$[W]$
r_n	Hydraulic radius of mine level n	$[m]$
z_n	Elevation of mine level n	$[m]$
τ_n^{air}	Air temperature on mine level n	$[^\circ C]$
α	Thermal diffusivity of the mine rock	$\left[\frac{m^2}{s}\right]$
ϵ_n	Thermal emissivity coefficient of mine level n	$[-]$
η_n	Age of airway for mine level n	$[s]$
τ_n^{v}	Virgin rock temperature on mine level n	$[^\circ C]$
ω_n	Goch-Patterson coefficient of mine level n	$[-]$
Physical Constants		
g	Acceleration due to gravity	$\left[\frac{m}{s^2}\right]$
∇^{T}	Thermal gradient	$\left[\frac{^\circ C}{m}\right]$

2.1 Heat from diesel equipment

Much of the heavy machinery necessary for ore extraction consumes diesel fuel and, correspondingly, emits a significant amount of heat into the air. In fact, diesel equipment can account for more than 50% of the heat production in underground operations, causing a non-trivial increase in the ambient air temperature (Bascompta et al. 2016).

Hot exhaust gases from the diesel equipment contain a significant portion of water vapor that impacts both the dry-bulb and the wet-bulb temperatures, the latter of which is calculated based on dry-bulb temperature and relative humidity. Government safety regulations for mine workers stipulate that operations must be halted when the wet-bulb temperature reaches $32.5^{\circ}C$ (Howes 2011). Each piece of diesel equipment has a specific set of cycle stages associated with the execution of an activity underground. (See Table 1 for an example related to a haul truck.) The heat load is estimated as the heat transfer rate from the diesel equipment to the environment and is determined by the engine motor load and the proportion of time the diesel equipment is running at each cycle stage.

The heat load of the associated diesel equipment can be estimated using a modeling software such as GT-SUITE (Gamma Technologies 2017), which is one-dimensional simulation software that employs fully unsteady nonlinear Navier-Stokes equations based on engine specifications and ambient conditions (see, e.g.,

Table 1 Engine load details for a representative haul truck

Cycle stage	Engine power load [%]	Proportion of time [%]
Up Ramp	100	40
On Surface	0	5
Down Ramp	10	35
Loading or Idling	10	20

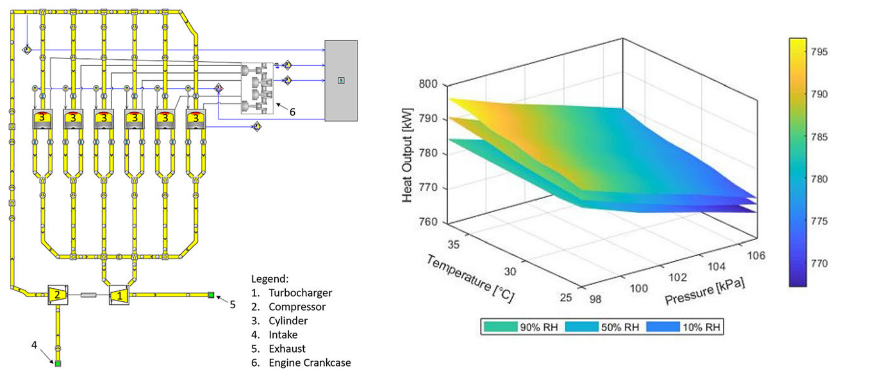

(a) An engine map used as an input in GT-SUITE for simulating heat emissions from a haul truck's diesel engine

(b) A depiction of a haul truck engine's heat output simulated in GT-SUITE and determined by pressure, ambient air temperature, and relative humidity (RH)

Fig. 4 Respective inputs and outputs modeled in GT-SUITE (Nichols et al. 2019)

Figure 4a for a haul truck). Figure 4b illustrates the effect of ambient temperature, humidity, and pressure on the heat load, using the haul truck as an example. As the diesel equipment operates deeper in the mine, the air temperature increases. Additionally, due to gravity, traveling deeper in the mine causes increased pressure. The combination of these factors, and changes in humidity, lower the performance of the engine, and increase the heat released into the environment, assuming a fixed mass of fuel consumed based on the maximum power calculations at standard temperature and pressure conditions (25°C and 101 kPa, respectively).

The output from GT-SUITE results in the heat load emitted from any given piece of equipment e in cycle stage c and based on the ambient environment conditions on mine level n, $\dddot{q}_{ecn}$. Calculating the total heat load associated with a piece of equipment e on mine level n, $\ddot{q}_{en}$, requires the proportion of time equipment e spends performing cycle stage c on level n, $\widehat{p}_{ecn}$, and is given as follows:

$$\ddot{q}_{en} \equiv \sum_{c \in \mathcal{C}_{en}} \widehat{p}_{ecn} \cdot \dddot{q}_{ecn} \quad \forall\ e \in \mathcal{E}, n \in \mathcal{N} \tag{1}$$

Due to the variability in activity type and duration, a proportion, $\hat{p}_{ea}$, is assigned to each piece of equipment e used for activity a to account for the appropriate amount of heat for each respective activity that could occur underground. Therefore, the heat load for each activity a is defined as follows:

$$\dot{q}_a \equiv \sum_{e \in \mathcal{E}_a} \hat{p}_{ea} \cdot \ddot{q}_{en} \quad \forall\ n \in \mathcal{N}, a \in \tilde{\mathcal{A}}_n \tag{2}$$

Although we provide a mathematical rendition of the heat as a function of equipment type on a given level, accounting for both the equipment and its location (level), in our computations, we remove the n index by using the assumption that the heat generated by the haul trucks on the ramps is negligible for the following reasons: *(i)* the amount of time that the truck is being used to execute an activity, and specifically, haul ore up a ramp, is 8% of the total time of the activity duration; *(ii)* when the truck is in transit, the airflow in the tunnels is significantly faster than the movement of the truck, obfuscating the heat being emitted by the truck; and *(iii)* generally speaking, there is simultaneous operation on only one to two levels, implying that any heat accumulation on other levels is irrelevant for mine worker conditions. Instead, we assign the heat output from the haul trucks entirely to the level on which the trucks "originate"; while we concede that this is an overestimation, we argue that we do account for all the heat in a linear fashion along the tunnel, which provides the best estimation with the available data (which excludes the haul paths).

2.2 Heat from auto-compression

Underground mining operations can exist at depths of up to 4,000 meters below the surface. Auto-compression indicates an increased temperature with this depth, and is caused by the conversion of potential energy into enthalpy directly linked to the elevation, z_n (Wagner 2013). Equation (3) relates the air temperature to the depth, provided the initial surface conditions are known:

$$\tau_n^{\mathrm{air}} = \tau_{n-1}^{\mathrm{air}} + g \cdot \frac{z_{n-1} - z_n}{c_p} \quad \forall\, n \in \mathcal{N} \tag{3}$$

Due to the six-degree change in temperature exhibited in the underground mine we use in our case study, implying that the change in specific heat capacity of air is less than 0.05%, we assume a constant value of $1{,}006 \frac{J}{kg \cdot {}^{\circ}C}$ based on initial surface dry-bulb temperature of $25^{\circ}C$. The air temperature due to auto-compression is calculated a priori and provided as a parameter, further discussed in Sect. 3.

2.3 Heat from strata rock

As new airways are created in an underground mine, the mine cavity itself gives off heat. Hartman et al. (2012) provide an equation calculating the heat load based on the excavated area for each mine level n:

$$\dot{q}_n^{\mathrm{v}} = l_n \cdot p_n \cdot \frac{k}{r_n} \cdot (\tau_n^{\mathrm{v}} - \tau_n^{\mathrm{air}}) \cdot \omega_n \quad \forall\, n \in \mathcal{N} \tag{4}$$

Thermal rock properties, such as k, are assumed to be known a priori and to be constant throughout the mine; the values are based on mine layout and infrastructure necessary for the geotechnical stability of the operation. Knowledge of the area and volumetric properties, such as length, perimeter and hydraulic radius of the mine level (l_n, p_n, and r_n, respectively), are provided by mine planners a priori and used in software such as Deswik (Deswik Mining Consultants (Australia) Pty Ltd 2018). The product of l_n and p_n produces the daily area advancement on mine level n. To calculate the virgin rock temperature, τ_n^{v}, the thermal gradient (∇^T) constant is necessary for all mine levels. The virgin rock temperature increases as elevation (denoted by z_n) decreases – similar to its relationship with auto-compression:

$$\tau_n^{\mathrm{v}} = \tau_{n-1}^{\mathrm{v}} + (z_{n-1} - z_n) \cdot \nabla^{\mathrm{T}} \quad \forall\, n \in \mathcal{N} \tag{5}$$

The Goch-Patterson coefficient, ω_n, is derived by interpolating the thermal emissivity coefficient, ϵ_n. Hartman et al. (2012) calculate ϵ_n using a collection of airway and thermal rock properties for each level n:

$$\epsilon_n = \frac{\alpha \cdot \eta_n}{r_n^2} \quad \forall\, n \in \mathcal{N} \tag{6}$$

Heat load from virgin rock, $\dot{q}_n^{\mathrm{v}}$, in equation (4), is used as a parameter and discussed further in Sect. 3. In our mathematical formulation of production scheduling that considers the presence of heat, we also allow for an option to mitigate it, namely through the use of refrigeration, which lowers the initial ambient air temperature and increases the maximum heat load allowed with respect to each mine level.

3 Ventilation formulation ($\mathcal{O}$)

We address the problem of determining, for an underground mine with a set of activities, which are selected, and when they are executed, and, correspondingly, when refrigeration is activated, to yield a production schedule that maximizes discounted net present value. The schedule adheres to temperature conditions by level as a function of the number of activities simultaneously executed in various active parts of a mine, precedence between activities, and resource constraints such as mill and extraction capacities. Our *original* formulation, ($\mathcal{O}$), subscribes to the following optimization modeling assumptions in addition to the thermal science assumptions given in Sect. 2: (*i*) Each activity requires at least one time period to execute; (*ii*) there is a constant mining rate; (*iii*) resources are consumed equally by a given activity over its duration; (*iv*) once refrigeration is activated, it must remain on for the remainder of the time horizon; and (*v*) parameters such as heat sources from strata rock and auto compression can be modeled as deterministic. Assumptions (*i*), (*ii*), and (*iii*) can be justified by ensuring that the mining operation is appropriately partitioned both temporally and spatially, respectively. Assumptions (*iv*) and (*v*) suffice for tactical mine planning for which refrigeration decisions are made at a coarse level, both spatially and temporally; the concluding section discusses an extension in which this is relaxed.

Symbol	Definition	Units
Simple sets		
$\mathcal{A}$	Activities	
$\mathcal{N}$	Mine levels	
$\mathcal{R}$	Production resources	
$\mathcal{S}$	Stages of refrigeration	
$\mathcal{T}$	Time periods	
Indexed sets		
$\tilde{\mathcal{A}}_n \subset \mathcal{A}$	Activities that occur on mine level n	
$\hat{\mathcal{A}}_r \subset \mathcal{A}$	Activities that consume production resource r	
$\mathcal{P}_a \subset \mathcal{A}$	Precedence activities for activity a	
Parameters		
c_p	Specific heat capacity of air	$\left[\frac{J}{kg \cdot {}^\circ C}\right]$
$\hat{d}_a$	Duration of activity a	[days]
$\bar{d}_{a'a}$	Delay between finishing activity a' and starting activity a	[days]
f	Fixed cost of refrigerated air	[$]
$\dot{m}_n$	Mass flow rate of air on mine level n	$[\frac{kg}{s}]$
p_a	Net present value derived from performing activity a	[$]
$\dot{q}_a$	Heat load for activity a	$[W]$
$\dot{q}_n^{\text{v}}$	Virgin rock heat load on mine level n	$[W]$
r_{ar}	Amount of production resource r required for activity a	[tons, meters, –]
$\hat{r}_{rt}$	Amount of production resource r available in time period t	[tons, meters, –]
δ	Daily discount rate	[-]
κ	Operation and maintenance cost of refrigeration	[$]

Symbol	Definition	Units
$\bar{\tau}_n$	Maximum air temperature allowed on mine level n	$[^{\circ}C]$
τ_n^{air}	Air temperature on mine level n based on auto-compression	$[^{\circ}C]$
τ_s^{cold}	Refrigerated air temperature at the surface for stage s	$[^{\circ}C]$
τ_{sn}^{mix}	Air temperature with refrigeration at stage s on level n	$[^{\circ}C]$
ϕ^{air}	Volumetric portion of ambient air mixed at the surface	[–]
ϕ^{cold}	Volumetric portion of refrigerated air mixed at the surface	[–]
Continuous variables		
$\tilde{H}_{nt}$	Net heat load on mine level n during time period t	$[W]$
F_{nt}	Final air temperature on mine level n at time period t	$[^{\circ}C]$
Binary variables		
Y_{at}	1 if activity a starts in time period t, 0 otherwise	[binary]
$\hat{Z}_{st}$	1 if refrigerated air of stage s is activated by time period t, 0 otherwise	[binary]

$$(\mathcal{O}) \quad \max \quad \sum_{t \in \mathcal{T}} \left(\frac{1}{1+\delta} \right)^t \cdot \left(\sum_{a \in \mathcal{A}} p_a \cdot Y_{at} - \sum_{s \in \mathcal{S}} \left(f \cdot (\hat{Z}_{st} - \hat{Z}_{s,t-1}) + \kappa \cdot \hat{Z}_{st} \right) \right) \tag{7a}$$

subject to:

$$\sum_{t' \leq t} Y_{at'} \leq \sum_{t'=1}^{t-\bar{d}_{a'a}-\hat{d}_{a'}} Y_{a't'} \quad \forall\, a \in \mathcal{A}, a' \in \mathcal{P}_a, t \in \mathcal{T} \tag{7b}$$

$$\sum_{t \in \mathcal{T}} Y_{at} \leq 1 \quad \forall\, a \in \mathcal{A} \tag{7c}$$

$$\sum_{a \in \hat{\mathcal{A}}_r} \sum_{t'=t-\hat{d}_a+1}^{t} \frac{r_{ar}}{\hat{d}_a} \cdot Y_{at'} \leq \hat{r}_{rt} \quad \forall\, r \in \mathcal{R}, t \in \mathcal{T} \tag{7d}$$

$$\tilde{H}_{nt} = \dot{q}_n^{\text{v}} + \sum_{a \in \tilde{\mathcal{A}}_n} \sum_{t'=t-\hat{d}_a+1}^{t} \frac{\dot{q}_a}{\hat{d}_a} \cdot Y_{at'} \quad \forall\, n \in \mathcal{N}, t \in \mathcal{T} \tag{7e}$$

$$\begin{aligned} \tilde{H}_{nt} = \dot{m}_n \cdot c_p \cdot \Big(& F_{nt} - \tau_n^{\text{air}} \cdot (1 - \hat{Z}_{1t}) \\ & - \sum_{s \in \mathcal{S}: s<1} \tau_{s-1,n}^{\text{mix}} \cdot (\hat{Z}_{s-1,t} - \hat{Z}_{st}) - \tau_{|\mathcal{S}|n}^{\text{mix}} \cdot \hat{Z}_{|\mathcal{S}|t} \Big) \quad \forall\, n \in \mathcal{N}, t \in \mathcal{T} \end{aligned} \tag{7f}$$

$$\hat{Z}_{st} \leq \hat{Z}_{s-1,t} \quad \forall\, s \in \mathcal{S} : s > 1, t \in \mathcal{T} \tag{7g}$$

$$\hat{Z}_{s,t-1} \leq \hat{Z}_{st} \quad \forall\, s \in \mathcal{S}, t \in \mathcal{T} : t > 1 \tag{7h}$$

$$0 \leq F_{nt} \leq \bar{\tau}_n \quad \forall\, n \in \mathcal{N}, t \in \mathcal{T} \tag{7i}$$

$$\tilde{H}_{nt} \text{ unrestricted} \quad \forall n \in \mathcal{N}, t \in \mathcal{T} \tag{7j}$$

$$Y_{at} \text{ binary} \quad \forall\, a \in \mathcal{A}, t \in \mathcal{T} \tag{7k}$$

$$\hat{Z}_{st} \text{ binary} \quad \forall\, s \in \mathcal{S}, t \in \mathcal{T} \tag{7l}$$

The objective function (7a) maximizes the discounted net present value based on the execution time of an activity a and the cost of refrigerated air. Constraint (7b) ensures precedence activities, $a' \in \mathcal{P}_a$, of activity a are completed before said activity can start. Constraint (7c) restricts all activities $a \in \mathcal{A}$ to at most one start time across the entire horizon $t \in \mathcal{T}$. Constraint (7d) limits the number of activities, $a \in \hat{\mathcal{A}}_r$, that can start in time period t based on each production resource limit $\hat{r}_{rt}$; these resources do not include allowable heat, but rather, the following two constraints accommodate this. Specifically, Constraint (7e) monitors the net heat load present from the strata and activities occurring on mine level n, which can be thought of as a "ventilation domain" with its own mass flow rate; this parameter is used specifically in Constraint (7f), which computes the net heat load from the temperature of the air flowing in and out of a mine level while also considering refrigeration, where the "by" definition of variable $\hat{Z}_{st}$ simplifies the expression on the right-hand side owing to the requirement that, once activated, refrigeration remains on for the duration of the mine life. The initial mixed air temperature at the surface is calculated as follows:

$$\tau^{\text{mix}}_{s,\text{surface}} = \phi^{\text{air}} \cdot \tau^{\text{air}}_{\text{surface}} + \phi^{\text{cold}} \cdot \tau^{\text{cold}}_{s} \quad \forall\, s \in \mathcal{S} \tag{8}$$

We assume the volumetric portion of refrigerated air and ambient air is mixed equally ($\phi^{\text{air}} = \phi^{\text{cold}} = 0.50$) at the surface and is sent down to the corresponding levels. The temperature of the mixed air increases as the air travels deeper into the mine due to auto-compression. The corresponding temperature is calculated similar to the way in which the ambient air temperature for mine level n is computed in equation (3):

$$\tau^{\text{mix}}_{sn} = \tau^{\text{mix}}_{s,n-1} + g \cdot \frac{z_{n-1} - z_n}{c_p} \quad \forall\, s \in \mathcal{S}, n \in \mathcal{N} \tag{9}$$

Constraint (7g) enforces precedence structure of the refrigeration stages. Constraint (7h) maintains refrigeration for the remainder of the horizon once active. Constraint (7i) ensures non-negativity and an upper bound on the final temperature at time period t on mine level n, i.e., it restricts the temperature in a domain. Finally, constraints (7k) and (7l) enforce binary requirements. Figure 5 provides a visual depiction of how these components produce an optimal schedule.

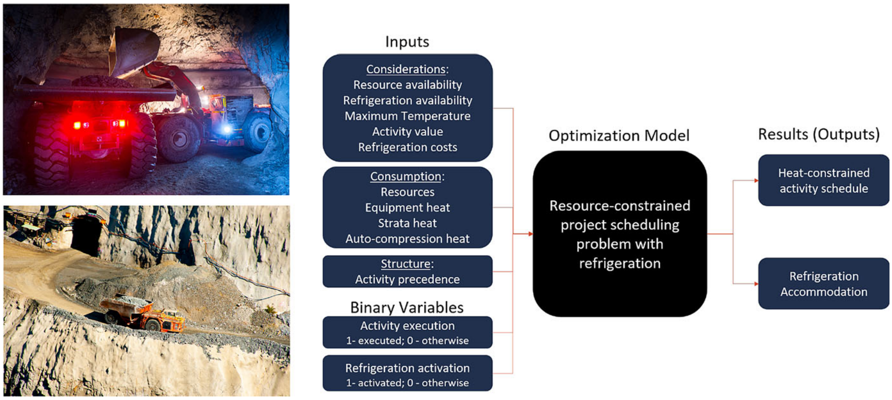

Fig. 5 Activities such as loading (top-left: Agnor (2017)) and hauling ore (bottom-left: Adwo (2020)) combine to produce an optimal heat-constrained production schedule considering ventilation and refrigeration (flowchart on right)

4 Solution methodology

State-of-the-art integer-programming solvers such as CPLEX (ILOG IBM 2019) have difficulty generating solutions for realistic instances of formulation ($\mathcal{O}$), even to within 10% of optimality in a reasonable amount of time. Many heuristics have been applied to mine planning problems with mathematical structure similar to ours. For example, O'Sullivan and Newman (2014) separate the monolith into several sub-problems associated with the value of ore, and solve these sub-problems, decreasing by block size. An alternative divides the problem temporally, rather than spatially, using a sliding time window that can accommodate discrete decisions in the shorter term while relaxing variables representing decisions more distant in time to be continuous, and/or not considering them at all (Lopes 2017). However, there is no guarantee of optimality using either of these approaches; in fact, a monolithic solve that would provide a bound on the solution quality is elusive using standard approaches. By reformulating our model as a *resource-constrained project scheduling problem* (RCPSP), we can exploit its special structure not only to obtain a solution to the linear programming relaxation of the problem (Bienstock and Zuckerberg 2010) but also to use this solution to generate a good, integer-feasible solution to the monolith. See Muñoz (2012) for details.

4.1 Reformulation of ($\mathcal{O}$)

The RCPSP contains three types of constraints: (*i*) precedence (Constraint (7b)), (*ii*) unique activity start time (Constraint (7c)), and (*iii*) resource knapsacks (Constraint (7d)). For ease of implementation in the solver, i.e., OMP (Rivera et al. 2016), we use the "at" (rather than the "by") variable definitions. To this end, we define the following additional notation for reformulation ($\mathcal{R}^+$):

Symbol	Definition	Units
Parameters		
$\bar{h}_n$	Upper heat load limit for level n	[W]
g_{sn}	Cooling load of stage s for level n	[W]
Binary variable		
Z_{st}	1 if refrigerated air of stage s is activated at time period t, 0 otherwise	[binary]

$$(\mathcal{R}^+)\quad \max \quad \sum_{t\in\mathcal{T}}\left(\frac{1}{1+\delta}\right)^t\cdot\left(\sum_{a\in\mathcal{A}}p_a\cdot Y_{at}-\sum_{s\in\mathcal{S}}\big(f+\kappa\cdot(|\mathcal{T}|-t)\big)\cdot Z_{st}\right) \tag{10a}$$

subject to:

(7b); (7c); and (7d)

$$\sum_{s\in\mathcal{S}}\sum_{\hat{t}=1}^{t}g_{sn}\cdot Z_{s\hat{t}}+\sum_{a\in\tilde{\mathcal{A}}_n}\sum_{t'=t-\hat{d}_a+1}^{t}\frac{\dot{q}_a}{\hat{d}_a}\cdot Y_{at'}\leq\bar{h}_n \quad \forall\, n\in\mathcal{N}, t\in\mathcal{T} \tag{10b}$$

$$\sum_{\hat{t}=1}^{t}Z_{s\hat{t}}\leq\sum_{\hat{t}=1}^{t}Z_{s-1,\hat{t}} \quad \forall\, s\in\mathcal{S}:s>1, t\in\mathcal{T} \tag{10c}$$

$$\sum_{t\in\mathcal{T}}Z_{1t}\leq 1 \tag{10d}$$

(7k) and (7l)

In formulation ($\mathcal{R}^+$), the variable Z_{st} undergoes a structural change (see, e.g., Lambert et al. (2014) for more detail). Constraints (7b), (7c), and (7d) are retained. Constraints (7e) and (7f) are reformulated, eliminating variables $\tilde{H}_{nt}$ and F_{nt}. Constraint (10b) is a relaxed heat resource knapsack that incorporates parameters $\bar{h}_n$ and g_{sn} to account for refrigeration for any given mine level n. Specifically, the upper heat load limit, $\bar{h}_n$, is defined as:

$$\bar{h}_n=\dot{m}_n\cdot c_p\cdot(\bar{\tau}_n-\tau_n^{\text{air}})-\dot{q}_n^{\text{v}} \quad \forall\, n\in\mathcal{N} \tag{11}$$

where the expression follows from algebraic manipulations on (7e) and (7f) and the substitution of $\bar{\tau}_n$ for F_{nt}, and is valid because of the inequality in (10b). Equation (11) considers the heat load from the virgin rock, $\dot{q}_n^{\text{v}}$, and uses the ambient air temperature due to auto-compression as an initial temperature on mine level n to inform the maximum allowable heat load on any given level. The cooling load, g_{sn}, for each stage s and mine level n is calculated as:

$$g_{1n} = \dot{m}_n \cdot c_p \cdot (\tau^{\text{mix}}_{1n} - \tau^{\text{air}}_n) \quad \forall n \in \mathcal{N} \tag{12}$$

$$g_{sn} = \dot{m}_n \cdot c_p \cdot (\tau^{\text{mix}}_{sn} - \tau^{\text{mix}}_{s-1,n}) \quad \forall n \in \mathcal{N}, s \in \mathcal{S} : s > 1 \tag{13}$$

where the expressions follow owing to algebraic manipulations similar to those used to derive (11).

Due to the transformation of Z_{st}, Constraints (7g) and (7h) are transformed into Constraints (10c) and (10d) to represent the precedence structure of refrigeration stages $s \in \mathcal{S}$ for all time periods $t \in \mathcal{T}$. Constraints (7i) and (7j) are removed due to the excision of F_{nt} and $\tilde{H}_{nt}$. The revised formulation ($\mathcal{R}^+$) is structured as an RCPSP. Therefore, we can use the special-purpose, fast solver OMP to generate solutions to its linear programming relaxation.

4.2 Propagated early start algorithm

The propagated early start algorithm is an in-built feature of the software we use, and reduces the number of activity-start time combinations (and, hence, Y_{at} variables) based on the precedence structure between activities (including lag times between the completion of one activity and the start time of a successor), and their durations. The set of activities can be visualized as nodes on a graph, and the arcs connecting them denote precedence. Given this, it is possible to traverse the graph in a topologically sorted order and assign to each activity an earliest start time. Any activity without predecessors possesses an early start time corresponding to the first period in the horizon. For any activity with one or more predecessors, the early start is determined by the most constraining time of any predecessor, given as the sum of: (*i*) the earliest time at which said predecessor can finish and any lag time between the end of that predecessor activity and (*ii*) the start time of a successor. The propagated early start algorithm helps enhance tractability; variants of this algorithm relying on precedence and resource constraints have been employed in other mining settings, e.g., Martinez and Newman (2011).

4.3 Optimization-based heuristic ($\mathcal{H}$)

Given a solution to the linear programming relaxation, (Y', Z'), of formulation ($\mathcal{R}^+$), we construct a corresponding integer-feasible solution by sequentially running the simple sorting algorithm (ALGORITHM 1), and the topological sorting algorithm (ALGORITHM 2).

First, ALGORITHM 1 determines the set of activities $\mathcal{A}' \subseteq \mathcal{A}$ that should potentially be scheduled. Specifically, set $\mathcal{A}'$ is defined as follows:

$$\mathcal{A}' \equiv \{a \in \mathcal{A} : \sum_{t \in \mathcal{T}} Y'_{at} > 0\} \tag{14}$$

Then, ALGORITHM 1 sorts activities, non-decreasing by their respective *mean start times*. We define the mean start time M_a for each activity $a \in \mathcal{A}$ as follows:

$$M_a \equiv \sum_{t \in \mathcal{T}} t \cdot Y'_{at} \tag{15}$$

Second, ALGORITHM 2 determines, for each stage, at what period refrigeration is activated, and then schedules the activities in topological order. Given a stage s, the time period $\tilde{t}_s$ at which the refrigeration starts is determined as follows:

$$\tilde{t}_s \equiv \min_{t \in \mathcal{T}} \{\sum_{t'=1}^{t} Z'_{st'} \geq \alpha\} \tag{16}$$

where $\alpha \in \mathbb{R}$ is a parameter such that $0 \leq \alpha \leq 1$. This parameter represents a threshold value associated with refrigeration start time; larger values for α correspond to later start times.

ALGORITHM 2 repeatedly determines the refrigeration and activity start times for different values of α, and then chooses the best solution. For example, let us assume three alternative values for α: 0.85, 0.9, or 0.95. In this case, ALGORITHM 2 determines three solutions, each of which corresponds to a given value of α; it then chooses the best solution among the three determined by their respective objective function values. The list that contains the values of α corresponds to *α_points*.

Algorithm 1: SIMPLE SORT

Data: Solution Y' from having solved the linear relaxation of formulation ($\mathcal{R}^+$)

Result: Sorted list of activities L

1 construct set $\mathcal{A}'$ of activities that will potentially be executed: $\mathcal{A}' \leftarrow \{a \in \mathcal{A} : \sum_{t \in \mathcal{T}} Y'_{at} > 0\}$;

2 compute mean starting time M_a of each activity $a \in \mathcal{A}'$: $M_a \leftarrow \sum_{t \in \mathcal{T}} t \cdot Y'_{at}$;

3 sort activities in set $\mathcal{A}'$, non-decreasing by M_a and assign to ordered list L;

4 **return** list L;

Algorithm 2: TOPOLOGICAL SORT

Data: List of activities L and solution (Y', Z') from having solved the linear relaxation of formulation $(\mathcal{R}^+)$
Result: Feasible solution $(Y^{\text{best}}, Z^{\text{best}})$ to formulation $(\mathcal{R}^+)$

$v^* \leftarrow -\infty$;
foreach $\alpha \in \alpha\_points$ **do**
  $Y_{at} \leftarrow 0$ for each activity $a \in \mathcal{A}$, time period $t \in \mathcal{T}$;
  foreach *stage* $s \in \mathcal{S}$ **do**
    $Z_{st} \leftarrow 0$ for time period $t \in \mathcal{T}$;
    $\tilde{t}_s \leftarrow \min_{t \in \mathcal{T}} \{\sum_{t'=1}^{t} Z'_{st'} \geq \alpha\}$;
    $Z_{s\tilde{t}_s} \leftarrow 1$;
  end
  while *list L is not empty* **do**
    select the first activity a in list L and delete it from L;
    foreach *time period* $t \in \mathcal{T}$ **do**
      if *assigning Y_{at} to 1 is precedence-, resource-, and heat-feasible* **then**
        $Y_{at} \leftarrow 1$;
        break;
      end
    end
  end
  compute objective function value of solution (Y, Z) and save it in v;
  if $v > v^*$ **then**
    $v^* \leftarrow v$;
    $(Y^{\text{best}}, Z^{\text{best}}) \leftarrow (Y, Z)$;
  end
end
return feasible solution $(Y^{\text{best}}, Z^{\text{best}})$;

5 Results

We use data from a large-scale underground hardrock mining operation in which ore is extracted via a combination of sublevel stoping and sublevel caving. We solve formulation $(\mathcal{R}^+)$ using a direct interface of our model with OMP v20190809 on a Dell Poweredge R610 with Two Hex Core Intel Xeon x5670s running at 2.93 GHz, using 128 GB RAM, and possessing 1 TB HDD. The computational results: *(i)* illustrate the usage of diesel equipment; *(ii)* enhance model tractability in terms of solution time and quality of solutions found; and, *(iii)* demonstrate the practical benefits of and economic trade-offs associated with the exclusion of heat constraints, and the incorporation of refrigeration as a means to recover production when heat constraints are imposed. Table 2 defines the different formulations we test.

Table 2 Various formulations used to examine the quality of production schedules

Formulation	Mathematical description	Characteristics
$(\mathcal{R}^-)$	$(\mathcal{R}^+)$ without constraint (10b)	Omits consideration of heat (typical formulation)
$(\mathcal{R})$	$(\mathcal{R}^+)$ without variable Z_{st}	Constrains heat while precluding refrigeration (simplistic fix to typical formulation)
$(\mathcal{R}^+)$	Our formulation	Constrains heat while allowing for refrigeration (proposed)

5.1 Equipment overview

The underground mining operation we model utilizes a mixed equipment fleet of 70% diesel and 30% electric, averaged across all the operational hours of the anticipated set of activities to be scheduled over the planning horizon. Figure 6 shows the percentage of operational hours for equipment associated with activities underground.

5.2 Computation

The activity layout of the hard rock mining operation is produced by the mining software DESWIK (Deswik Mining Consultants (Australia) Pty Ltd 2018); see Fig. 7. Information regarding the *(i)* resource, e.g., grade, tons, linear feet, *(ii)* precedence, and *(iii)* location of each individual activity is exported for use in $(\mathcal{R}^+)$. The heat modeled by GT-SUITE is entered as data for the respective activities in DESWIK. As a means to simplify the formulation $(\mathcal{R}^+)$ and due to the mathematical structure required by OMP at the time of this writing, we assume an initial surface temperature of $25^\circ C$ and 80% relative humidity to be constant for the time horizons we consider

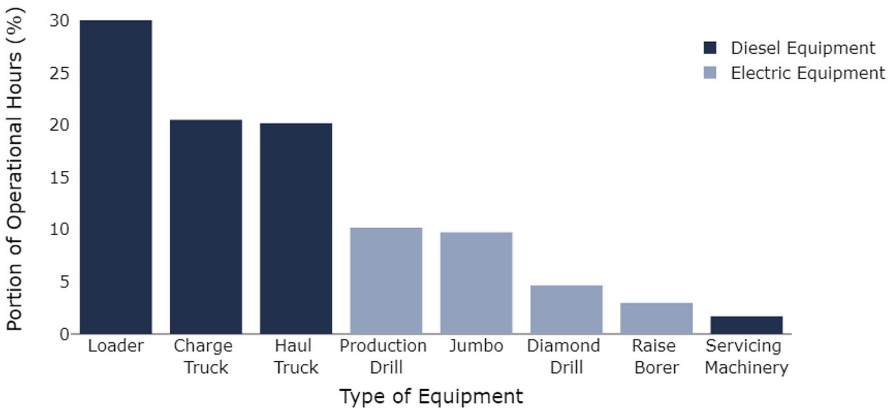

Fig. 6 Percentage of usage for each type of equipment

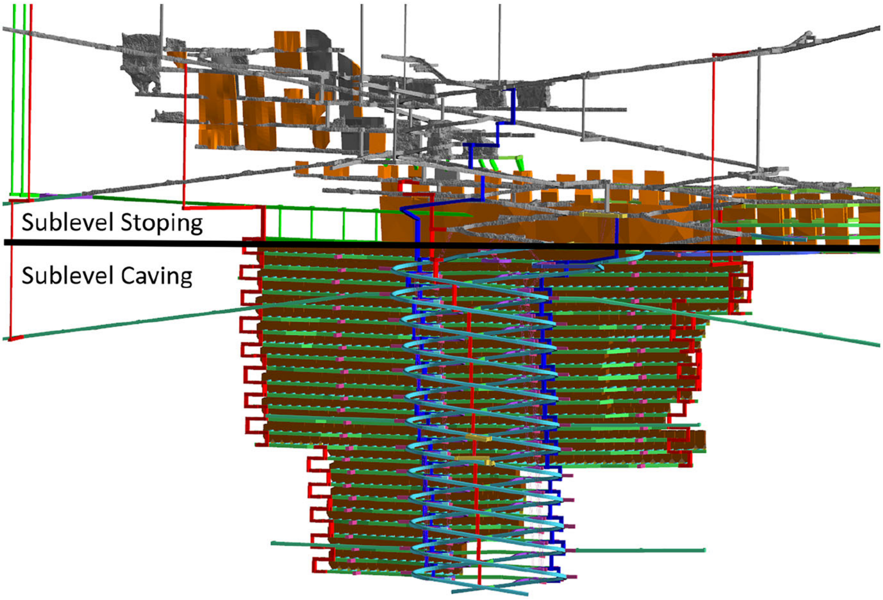

Fig. 7 The relevant area of the mine, which is comprised of a mixture of sublevel stoping and sublevel caving, in which the former occurs above the black horizontal line, while the latter is executed below the black horizontal line

based on weather station data provided by industry partners at the mining location. This assumption is considered sufficient for tactical scheduling.

Table 3 highlights the ten instances we schedule, which contain between 895 and 7,356 activities over a horizon consisting of between 365 and 913 days. Each

Table 3 Problem instances highlighting the number of total activities, stoping activities, caving levels, and horizons lengths

Case	Number of			
	Total activities	Stoping activities	Caving Levels	Horizon [days]
1	896	611	–	365
2	1522	1062	–	365
3	2271	380	1	365
4				548
5	2953	1062	1	365
6				548
7	6883	589	2	730
8				913
9	7356	1062	2	730
10				913

Table 4 Solution details of the respective cases

Case	Variable count		Refrigeration Activation [day]	Solution Time [seconds]*	Optimality Gap [%]
	Theoretical	Practical†			
1	731,798	491,358	–	14	0.35
2	960,806	620,912	8	252	15.34
3	1,235,689	661,226	84	165	7.97
4	2,154,900	1,328,460	82	634	12.89
5	1,485,616	827,792	86	745	9.49
6	2,530,000	1,619,000	89	2886	6.47
7	6,643,632	4,309,290	123	10,374	2.83
8	8,806,875	6,021,072	129	12,297	5.12
9	6,989,868	4,592,126	65	16,900	3.15
10	9,989,970	6,390,467	130	25,480	4.10

*Solution time includes linear programming relaxation and heuristic ($\mathcal{H}$) solve time

†Variable count representative of early start pre-processing

problem instance is differentiated by the nature of stoping activities, the location of caving level access, and/or the horizon length.

For each instance, we consider the option to activate a single stage of refrigeration. Due to tractability issues, CPLEX 12.10 is unable to determine feasible solutions, even for the smallest case, in a reasonable amount of time; Case 1 results in optimality gaps of 10% after 70,225 seconds, and refrigeration is not activated. Therefore, we employ the specialized solver OMP to determine better-quality solutions to larger instances within an acceptable amount of run time. Table 4 details these results with respect to *(i)* size of each instance, *(ii)* the time at which refrigeration is activated during the schedule, *(iii)* the resulting solution time after solving the linear program to optimality and employing heuristic ($\mathcal{H}$), and *(iv)* the resulting optimality gap. The solver's propagated early starts reduce the theoretical problem size by about 37%, on average. Refrigeration is activated in all but the smallest instance, and at varying times during the horizon. Solution times range from between a few seconds to eight hours, where longer solution times generally correspond to larger instances. On average, the time spent solving the linear programming relaxation constitutes 95% of the solution time; heuristic ($\mathcal{H}$) accounts for the other 5%. Gaps fall under 10% for all but two instances, averaging 5% for these eight. Two instances have larger gaps (about 12% and 15%) particularly due to the ability of the linear programming relaxation to activate only a small portion of refrigeration and, commensurately, to incur small costs; however, given that the instances are unsolvable in their monolithic instantiations, even these results represent significant improvements.

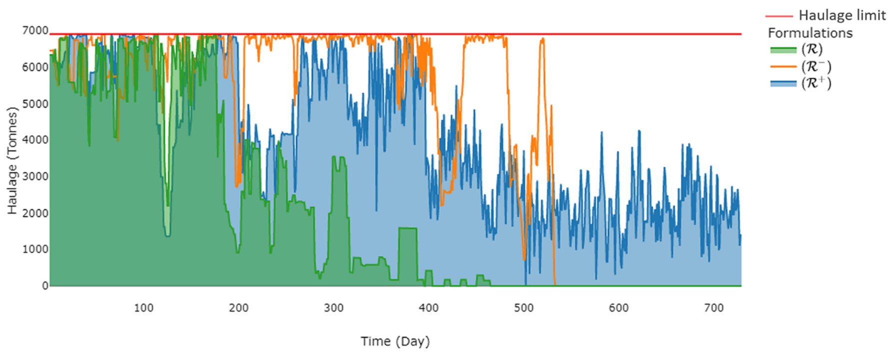

Fig. 8 Comparison of the respective formulations based on daily haulage, where $(\mathcal{R}^-)$ is the standard formulation, $(\mathcal{R})$ is the simplistic fix to formulation $(\mathcal{R}^-)$, and $(\mathcal{R}^+)$ is the proposed formulation

5.3 Managerial insights

The results from solving all formulation variants listed in Table 3 provide insights to mine planners. For long- and medium-term scheduling such as the situation we consider, the objective function maximizes net present value. A proxy for net present value is total daily haulage, because the tons extracted from the mine are subsequently sent to processing (without the intermediate stage of a stockpile, which is generally absent in underground mining), after which the product is sold. The hauled tons are typically the constraining factor in underground mines because of the rate of production relative to the rate at which other activities (such as blasting or backfilling) occur. For Case 7, Figure 8 presents the tons hauled, which acts as the limiting factor in at least some of the time periods over the course of the horizon. However, for the variant in which heat is not constrained, the tons hauled appears to be the limiting factor most of time; this suggests unreasonably high production levels and correspondingly unacceptably high temperatures. At the opposite extreme, the formulation in which we constrain heat but preclude refrigeration exhibits the fewest tons hauled, indicating that without the option to cool the mine, the schedule results in less extracted material, lowering the net present value. Employing the option of refrigeration mitigates heat levels while maintaining a fairly high production rate, and represents the most realistic, yet opportunistic, situation. Table 5 summarizes.

Figures 9 and 10 evaluate the temperature on the deepest mine level. The solution obtained with $(\mathcal{R}^-)$ for Case 7 violates the typical maximum temperature for normal

Table 5 Comparison of Case 7 formulations and their respective net present value changes

Formulation	Net present value change with respect to the objective value of $(\mathcal{R}^-)$ [%]	Feasibility with respect to temperature
$(\mathcal{R}^-)$	–	No
$(\mathcal{R})$	−42.30	Yes
$(\mathcal{R}^+)$	−12.29	Yes

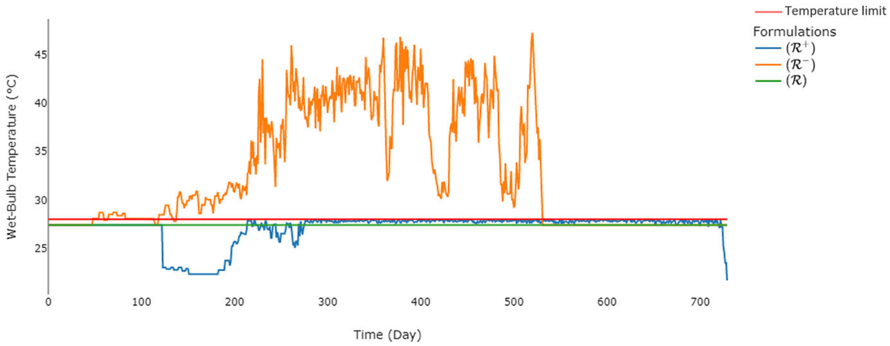

Fig. 9 Comparison of the respective formulation types based on end-of-day temperature outputs on the lowest level of the mine, where $(\mathcal{R}^{-})$ is the standard formulation, $(\mathcal{R})$ is the simplistic fix to formulation $(\mathcal{R}^{-})$, and $(\mathcal{R}^{+})$ is the proposed formulation

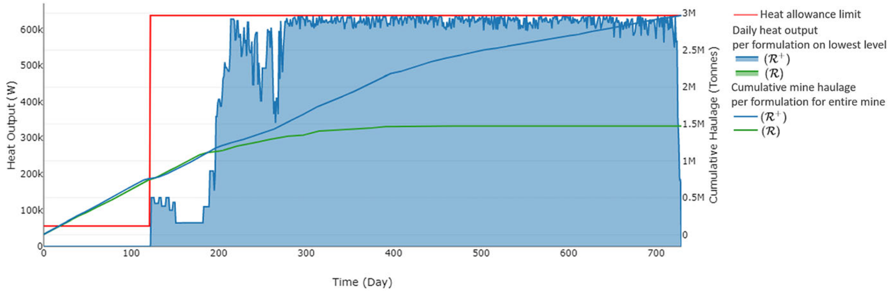

Fig. 10 Comparison of the heat-feasible schedules based on daily heat output on the lowest level in the mine, as well as on cumulative mine haulage for the entire mine, where $(\mathcal{R})$ is the simplistic fix to formulation $(\mathcal{R}^{-})$, and $(\mathcal{R}^{+})$ is the proposed formulation

operation, here $28°C$ wet-bulb; formulations $(\mathcal{R})$ and $(\mathcal{R}^{+})$ adhere to the heat limits. Without refrigeration, the mine level is too hot to operate; correspondingly, there are no executed activities on this level in $(\mathcal{R})$'s schedule (as suggested by the relatively flat portion of the curve after day 300 when the ability to execute activities on the higher levels is virtually exhausted). The refrigeration option exercised in formulation $(\mathcal{R}^{+})$'s schedule lowers the temperature; at the extreme, on day 123 when refrigeration is activated, there is a significant drop in temperature, which remains low until sufficient heat-generating activities are introduced into the schedule.

Comparing the formulations that produce the two feasible schedules – $(\mathcal{R}^{+})$ and $(\mathcal{R})$, the former possesses an advantage over the latter in that the increase of the right-hand side by over 580,000 W when refrigeration is activated on day 123 permits greater cumulative haulage for the entire mine, leading to a higher net present value, even though refrigeration costs are incurred.

6 Conclusions and future research directions

Underground mine planning is a complex process, critical to providing solutions that appropriately determine realistic execution dates of activities. We provide a detailed mixed integer programming formulation ($\mathcal{O}$) of a production scheduling problem that maximizes net present value by considering precedence, resources, and final temperature, where the latter feature is based on heat output at the end of each respective time period while incorporating refrigeration and ventilation at every mine level. We reformulate ($\mathcal{O}$) as ($\mathcal{R}^+$), which possesses a classical *RCPSP* structure; this enables us to solve large instances using a decomposition scheme for the linear programming relaxation and a tailored heuristic ($\mathcal{H}$) to produce integer-feasible solutions. For ten realistic test cases, we obtain solutions, on average, to within 7% of optimality in under two hours, where otherwise instances are intractable. Our solutions provide operationally feasible production schedules with respect to heat accumulation in an underground mine, while weighing the economic trade-offs between the cost incurred for activating refrigeration and the increased production enabled by it.

Future research could accommodate short-term scheduling by modifying ($\mathcal{O}$) and ($\mathcal{R}^+$) to incorporate transient effects, seasonal temperature and humidity variations, stochasticity associated with operational (e.g., equipment availability and associated production rate) and heat-source parameters, and financial and geotechnical uncertainty. Finally, our heuristic ($\mathcal{H}$) creates multiple solutions whose trade-offs could be evaluated by determining when refrigeration is activated.

Acknowledgements We acknowledge our industry partners who provided data, funding and an explanation of the scheduling problem. We thank Professor Marcos Goycoolea from the University of Adolfo Ibañez; Samuel Nichols, Kieran Lewis, Eric Smoorenberg, John Ayaburi, and Aditya Juganda from the Colorado School of Mines; and Akshay Chowdu from the South Dakota School of Mines for providing additional insights regarding model formulation. We also thank Dr. Mark Larson and Mr. Donovan Benton from the National Institute of Occupational Safety and Health for their constructive comments. This research has been partially funded by the National Institute of Occupational Safety and Health as part of the Mine Ventilation and Safety Research and Capacity Building program, contract number: 0000HCCS-2019-36404, and by the National Agency for Research and Development (ANID), Chile, Scholarship Program, Becas de Doctorado Nacional: 2017-21180460.

References

Acuña EI, Lowndes IS (2014) A review of primary mine ventilation system optimization. Interfaces 44(2):163–175

Adwo (2020) Mining truck driving out of underground mine [digital image]. Shutterstock, Accessed: 03/10/2021

Agnor M (2017) Gold mining underground [digital image]. Shutterstock, Accessed: 03/10/2021

Anderson J, Longson I (1986) Optimisation of ventilation and refrigeration in British coal mines. Min Eng 146:115–20

Atlas Copco (2007) Mining methods in underground mining. Stockholm: Atlas Copco

Bascompta M, Castañón AM, Sanmiquel L, Oliva J (2016) Heat flow assessment in an underground mine: an approach to improve the environmental conditions. Dyna 83(197):174–179

Bienstock D, Zuckerberg M (2010) Solving LP relaxations of large-scale precedence constrained problems. In: International Conference on Integer Programming and Combinatorial Optimization, Springer, pp 1–14

Both C, Dimitrakopoulos R (2020) Joint stochastic short-term production scheduling and fleet management optimization for mining complexes. Optim Eng, pp 1–27
Brake DJ, Fulker R (2000) The ventilation and refrigeration design for Australia's deepest and hottest underground operation: the Enterprise mine. Proc MassMin, pp 611–621
Brickey AJ (2015) Underground production scheduling optimization with ventilation constraints. PhD thesis, Colorado School of Mines. Arthur Lakes Library
Campeau LP, Gamache M (2020) Short-term planning optimization model for underground mines. Comput Op Res 115:104642
Carlyle M, Eaves C (2001) Underground planning at stillwater mining company. Interfaces 31(4):50–60
Carpentier S, Gamache M, Dimitrakopoulos R (2016) Underground long-term mine production scheduling with integrated geological risk management. Min Technol 125(2):93–102
Chowdu A, Nesbitt P, Brickey A, Newman A (2021) Operations research in underground mine planning: A review. INFORMS Journal on Applied Analytics, accepted
De Souza E (2007) Optimization of complex mine ventilation systems with computer network modelling. IFAC Proceedings Volumes 40(11):323–329, https://doi.org/10.3182/20070821-3-CA-2919.00049, URL https://www.sciencedirect.com/science/article/pii/S1474667015315597, 12th IFAC Symposium on Automation in Mining, Mineral and Metal Processing
Deswik Mining Consultants (Australia) Pty Ltd (2018) Deswik.CAD
Dimitrakopoulos R, Grieco N (2009) Stope design and geological uncertainty: quantification of risk in conventional designs and a probabilistic alternative. J Min Sci 45(2):152–163
Dirkx R, Kazakidis V, Dimitrakopoulos R (2019) Stochastic optimisation of long-term block cave scheduling with hang-up and grade uncertainty. Int J Min, Reclam Environ 33(6):371–388
Donoghue A (2004) Occupational health hazards in mining: an overview. Occup Med 54(5):283–289
Gamma Technologies (2017) GT-Power user's manual, GT-Suite version 2017. Gamma Technologies
Gertsch RE, Bullock RL (1998) Techniques in underground mining: selections from underground mining methods Handbook. Society for Mining Metallurgy and Exploration, Littleton
Greth A, Roghanchi P, Kocsis K (2017) A review of cooling system practices and their applicability to deep and hot underground U.S. mines. In: Proceedings of the 16th North American Mine Ventilation Symposium, Golden, CO, USA, pp 17–22
Hamrin H (1980) Guide to underground mining: methods and applications. Atlas Copco, Sweden
Hartman HL, Mutmansky JM (2002) Introductory Mining Engineering. Wiley, Hoboken
Hartman HL, Mutmansky JM, Ramani RV, Wang YJ (2012) Mine Ventilation and Air Conditioning. Wiley, Hoboken
Howes M (2011) Ventilation and cooling in underground mines. Min Quarr 74:45–46
Huang S, Li G, Ben-Awuah E, Afum BO, Hu N (2020a) A robust mixed integer linear programming framework for underground cut-and-fill mining production scheduling. Int J Min, Reclam Environ 34(6):397–414
Huang S, Li G, Ben-Awuah E, Afum BO, Hu N (2020b) A stochastic mixed integer programming framework for underground mining production scheduling optimization considering grade uncertainty. IEEE Access 8:24495–24505
Hustrulid WA, Bullock RC (2001) Underground mining methods: engineering fundamentals and international case studies. Society for Mining Metallurgy and Exploration, Littleton
ILOG IBM (2019) CPLEX optimizer 12.9
Jewbali J, Wang H, Johnson C (2015) Resource model uncertainty analysis and stope optimizer (MSO) evaluation for an underground metal mine project. In Application of Computers and Operations Research in the Mineral Industry. Society for Mining Metallurgy and Exploration, Littleton
Johnson TB (1968) Optimum open pit mine production scheduling. Tech. rep., DTIC Document
Khodayari F, Pourrahimian Y (2019) Long-term production scheduling optimization and 3D material mixing analysis for block caving mines. Min Technol 128(2):65–76
Kuchta M, Newman A, Topal E (2004) Implementing a production schedule at LKAB's Kiruna mine. Interfaces 34(2):124–134
Kutcha M, Newman AM, Topal E (2003) Production scheduling at LKAB's Kiruna mine using mixed-integer programming. Min Eng 55(4):35–40
Lambert B, Brickey A, Newman A, Eurek K (2014) Open-pit block-sequencing formulations: a tutorial. Interfaces 44(2):127–142
Larson M (2021) private communication
Lazaro P, Momayez M (2020) Development of a modified predicted heat strain model for hot work environments. Int J Min Sci Tech 30(4):477–481

Lerchs H, Grossmann IF (1965) Optimum design of open-pit mines. Trans CIM 58:47–54
Lopes TVF (2017) Underground mine production scheduling using OMP solver: Analysis of modifications to an integer programming model and implementation of a sliding time window heuristic. Master's thesis, South Dakota School of Mines and Technology, Rapid City
Magri E, Unsted A (1976) Mine production, ventilation and refrigeration planning-a unified approach via mathematical programming. International Federation of Automatic Control Proceedings Volumes 9(5):91–104
Marks JR (1980) Refrigeration economics at the Star mine. In Proceedings second international mine ventilation congress, SME, Littleton, CO, pp 649–655
Martinez M, Newman AM (2011) Using decomposition to optimize long- and short-term production scheduling at LKAB's Kiruna Mine. Euro J Op Res 211(1):184–197
Matamoros MEV, Dimitrakopoulos R (2016) Stochastic short-term mine production schedule accounting for fleet allocation, operational considerations and blending restrictions. Euro J Op Res 255(3):911–921
McPherson MJ (2009) Subsurface ventilation engineering. Mine Ventilation Services Inc., USA
McPherson MJ (2012) Subsurface ventilation and environmental engineering. Springer, Berlin
Mohtasham M, Mirzaei-Nasirabad H, Alizadeh B (2021) Optimization of truck-shovel allocation in open-pit mines under uncertainty: a chance-constrained goal programming approach. Min Techn 130(2): 81–100
Muñoz G (2012) Modelos de optimización lineal entera y aplicaciones a la minería. Master's thesis, Dept. Math. Engineering, Universidad de Chile, Santiago, Chile
Myers P, Standing C, Collier P, Noppe M (2005) Assessing underground mining potential at Ernest Henry Mine, using conditional simulation and stope optimisation. Orebody Model Strateg Mine Plan, Spectr Ser 14:141–180
Nehring M, Topal E, Kizil M, Knights P (2010) An investigation to integrate optimum long-term planning with short planning in underground mine production scheduling. In: Mine Planning and Equipment Selection Conference, Fremantle, Western Australia, pp 1–13
Nehring M, Topal E, Kizil M, Knights P (2012) Integrated short-and medium-term underground mine production scheduling. J South Afr Inst Min Metal 112(5):365–378
Nesbitt P, Blake LR, Lamas P, Goycoolea M, Pagnoncelli BK, Newman A, Brickey A (2021) Underground mine scheduling under uncertainty. Eur J Oper Res 294(1):340–352
Newman A, Kuchta M (2007) Using aggregation to optimize long-term production planning at an underground mine. Euro J Op Res 176(2):1205–1218
Newman A, Rubio E, Caro R, Weintraub A, Eurek K (2010) A review of operations research in mine planning. Interfaces 40(3):222–245
Nichols S, Bogin G, Newman A (2019) Simulation of the impact of environmental conditions in underground mines on truck and loader engine efficiency and emissions. In: SME Annual Conference & Expo and CMA 121st National Western Mining Conference, SME, pp 716–721
Nieto A (2011) Key deposit indicators (KDI) and key mining method indicators (KMI) in underground mining method selection. Trans Soc Min, Metal Eng 328:381–396
O'Sullivan D, Newman AM (2014) Extraction and backfill scheduling in a complex underground mine. Interfaces 44(2):204–221
O'Sullivan D, Brickey A, Newman A (2015) Is open pit production scheduling 'easier' than its underground counterpart? Min Eng 67(4):68–73
Rivera O, Brickey AJ, Espinoza D, Goycoolea M, Moreno E (2016) The OMP guide. In: Technical Report, Universidad Adolfo Ibañez
Rivera Letelier O, Espinoza D, Goycoolea M, Moreno E, Muñoz G (2020) Production scheduling for strategic open pit mine planning: a mixed-integer programming approach. Op Res 68(5):1425–1444
Sebutsoe T, Musingwini C (2017) Characterizing a mining production system for decision-making purposes in a platinum mine. J South Afr Inst Min Metal 117(2):199–206
Sharma V (2015) Longterm schedule optimization of an underground mine under geotechnical and ventilation constraints using SOT. PhD thesis, Laurentian University of Sudbury
Smith M, Sheppard I, Karunatillake G (2003) Using MIP for strategic life-of-mine planning of the lead/ zinc stream at Mount Isa mines. In: Proceedings of the 31st International APCOM Symposium, Cape Town, South Africa, pp 465–474
Sotoudeh F, Nehring M, Kizil M, Knights P, Mousavi A (2020) Production scheduling optimisation for sublevel stoping mines using mathematical programming: a review of literature and future directions. Resour Policy 68:101809

Tavchandjian O, Proulx A, Anderson M (2018) Application of conditional simulations to capital decisions for Ni-sulfide and Ni-laterite deposits. In: Advances in Applied Strategic Mine Planning, Springer, pp 319–333

Trout L (1995) Underground mine production scheduling using mixed integer programming. In: 25th International APCOM Symposium Proceedings, pp 395–400

Wagner H (2013) The management of heat flow in deep mines. Min Rep 149(2):88–100

Zhang H, Hauta R, Fava L (2017) Mine schedule optimisation with ventilation constraints: a case study. In: Proceedings of the First International Conference on Underground Mining Technology, Australian Centre for Geomechanics, pp 145–152

Authors and Affiliations

Oluwaseun Ogunmodede[1] · Patricio Lamas[2] · Andrea Brickey[3] · Gregory Bogin Jr.[1] · Alexandra Newman[1]

Oluwaseun Ogunmodede
oogunmod@mines.edu

Patricio Lamas
patricio.lamas@alicantolabs.com

Andrea Brickey
andrea.brickey@sdsmt.edu

Gregory Bogin Jr.
gbogin@mines.edu

[1] Colorado School of Mines, Golden, CO, USA

[2] Universidad Adolfo Ibáñez, Santiago, Chile

[3] South Dakota School of Mines, Rapid City, SD, USA